

N86-32991

INVESTIGATION OF LIMB-SIDESTICK DYNAMIC INTERACTION WITH ROLL CONTROL

Donald E. Johnston
Duane T. McRuer
Systems Technology, Inc.
13766 S. Hawthorne Blvd.
Hawthorne, CA 90250
(213)679-2281

ABSTRACT

A fixed-base simulation was performed to identify and quantify interactions between the pilot's hand/arm neuromuscular subsystem and such features of typical modern fighter aircraft roll rate command control system mechanizations as

- force sensing side-stick type manipulator
- vehicle effective roll time constant
- flight control system effective time delay

The simulation results provide insight to high frequency PIO (roll ratchet), low frequency PIO, and roll-to-right control and handling problems previously observed in experimental and production fly-by-wire control systems. The simulation configurations encompass and/or duplicate several actual flight situations, reproduce control problems observed in flight, and validate the concept that the high frequency nuisance mode known as "roll ratchet" derives primarily from the pilot's neuromuscular subsystem. The simulations show that force-sensing side-stick manipulator force/displacement/command gradients, command prefilters, and flight control system time delays need to be carefully adjusted to minimize neuromuscular mode amplitude peaking (roll ratchet tendency) without restricting roll control bandwidth (with resulting sluggish or PIO prone control).

The results further demonstrate that roll ratchet tendency, which is difficult to detect in fixed-base simulations, is readily apparent from application of frequency response spectral analysis techniques. Consequently the application of appropriate spectral measurement techniques during flight control system design/development piloted simulation phases promise to reduce later and more costly flight test investigation.

INTRODUCTION

✓ Almost every new aircraft with fly-by-wire or command augmentation (Fig. 1) in the roll axis has encountered either Pilot-Induced Oscillations (PIO) or roll ratcheting (or both) in early flight phases. PIO has typically been associated with high gain, neutrally stable closed-loop pilot-vehicle control oscillations with a frequency of about 1/2 Hz. The "roll ratchet" has been somewhat more obscure and idiosyncratic, appearing most often in rapid rolling maneuvers. Ratchet frequencies are typically 2-3 Hz.

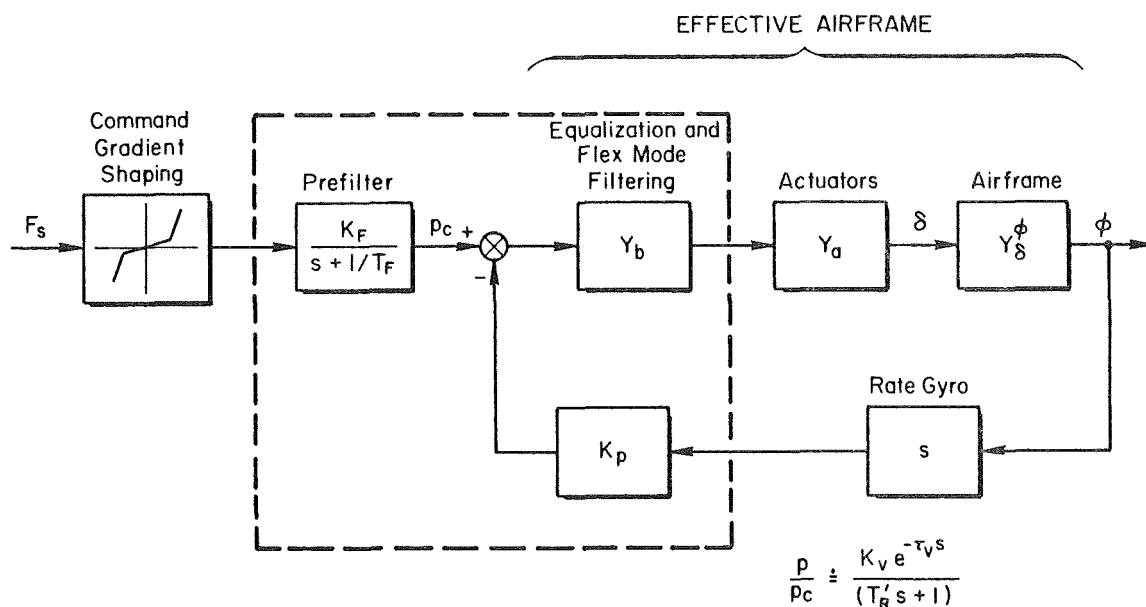


Figure 1. Typical Fly-by-Wire Roll Control System

Figure 2 illustrates this oft-remarked but seldom recorded phenomenon. The frequency difference alone indicates that the PIO and ratchet situations are different phenomena, yet both clearly involve the closed-loop pilot vehicle system.

An interesting set of roll ratcheting phenomena has been observed in variable stability NT-33 flight.²⁻⁴ Chalk⁵ speculates that the oscillations were due to the near K_c/s character of the effective controlled element. He used a rudimentary ($K_p e^{-\tau s}$) non-adaptive pilot model with τ ranging from 0.09 to 0.13 sec to show that one can get the observed instability (at about 12-17 rad/sec) with a K/s -like aircraft and high pilot gains. This effective time delay must account for all the open-loop system lags, i.e., controller, actuator, filters, etc., plus the effective latency of the pilot. So, if this explanation of the roll ratchet is to be reasonable the total τ value must be appropriate. The 0.09 - 0.13 second range is remarkably low for the pilot alone, and is very low indeed when aircraft plus control system effective lags are also considered.

Mitchell and Hoh¹ also examined some of the same data. They cite sinusoidal vibration data in which a simple lateral tracking task was performed (using a center stick) while under the influence of high frequency lateral accelerations.⁶ Frequencies from 1 to 10 Hz were employed and an oscillatory arm/stick "bobweight" mode occurred at about 12 rad/sec. They note that this higher frequency mode of the pilot-aircraft systems is near the frequencies of the observed ratcheting in F-16 and Calspan flight experiments and cite it as a possible cause.

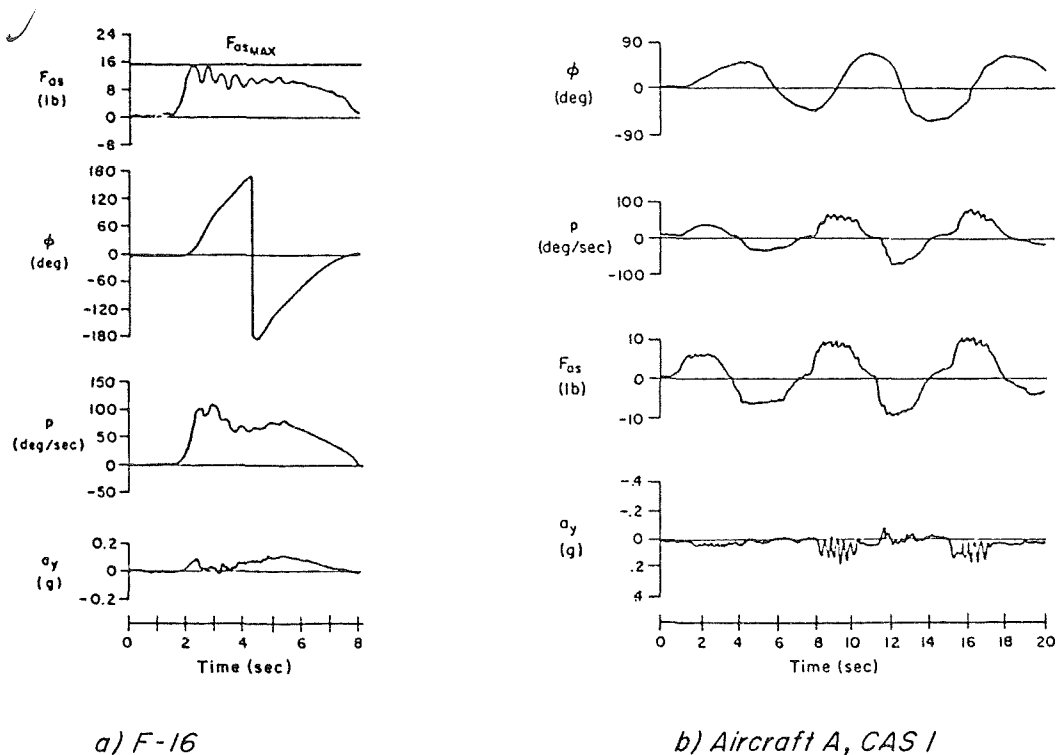


Figure 2. Roll Ratchet During Banking Maneuver

From the earliest studies on the interaction between the human pilot's neuromuscular system and aircraft control devices,^{7,8} the presence of a neuromuscular system limb-manipulator dynamic resonance peak at 14-19 rad/sec has been well known. Neuromuscular system characteristics are cited⁹ as "exceptionally important and critically limiting in such matters as

- control precision where limited by the pilot's neuromuscular system.
- effects of control system nonlinearities, including their connections with control system sensitivity requirements."

Other summaries place great stress on the importance of considering these characteristics even though this frequency range of major activity may be well above bandwidth associated with the "usual" control task.¹⁰

It is becoming more and more apparent that modern, high performance, high gain, response command flight control system bandwidths may be encroaching on the neuromuscular system. Advances in flight control system fly-by-wire technology permit new manipulation devices, for example force sensing side-sticks, at the pilot output/effective-vehicle interface. These have thus far been generally successful in application, but have introduced or enlarged some pilot-vehicle flying qualities problems. Particular problems include:^{2-4,11,12}

- high roll control sensitivity and PIO's in precision maneuvering;
- roll ratchet in otherwise steady rolling maneuvers;
- sensitivity to the way the pilot grips the stick or to location of his hand/arm support;
- effective time delay associated with stick filters, with attendant increase in pilot remnant;
- biodynamic interactions, e.g., hand/arm stick bob-weight effects.

Attempts to alleviate these effects have involved adjustments in stick force gradients, filtering, and sensitivity. These have included introduction of various nonlinear elements such as command gain reduction as a function of pilot input amplitude or frequency, filter time constant changes with sense of input (increase vs. decrease), and different force gradient for right and left roll commands. These adjustments have generally involved ad hoc empirical modifications in the course of the aircraft development. Much of this has been accomplished in flight test with correspondingly large cost.

The purposes of this paper are to

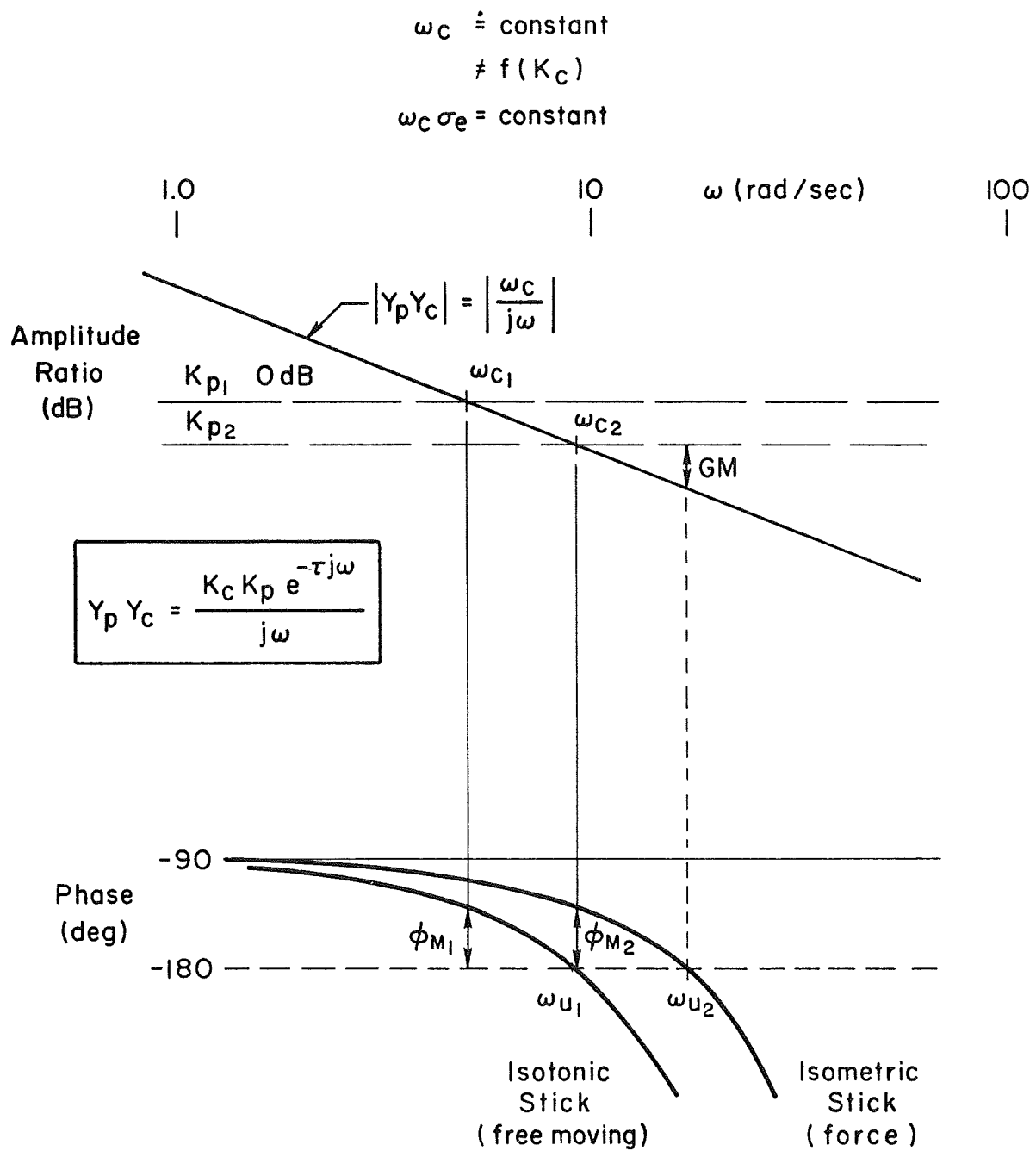
- explore the origins of the roll ratchet phenomenon;
- develop insights about the tradeoffs involved in adjusting the properties of force-sensing sidesticks;
- present guidelines to minimize roll control problems.

HUMAN PILOT-DYNAMIC SYSTEM CONSIDERATIONS

Ideal Crossover Model (and Its Implications)

The prescription for K/s-like controlled element dynamics in the region of pilot-vehicle system crossover as an often desirable form stems from the fundamental feature of human dynamics that no pilot lead is then required to establish good closed-loop system dynamics over a wide range of pilot gains. The basic recipe is almost invariably conditioned by such statements as "in the frequency region about crossover." Such statements are made to restrict the form of the pilot model to that required only in the crossover region. In particular, the cases covered are such that an effective time delay term in the pilot model is an adequate approximation to the high frequency effects.

Simple tracking task pilot model forms and associated pilot-vehicle system properties begin with the ideal crossover model¹⁰ of Fig. 3. In this model the pilot adjusts his dynamic characteristics so that the open-loop pilot-vehicle dynamics are approximately K/s over the frequency band immediately above and below the gain crossover. The model also indicates that in



$$\Delta\tau = \tau_{\text{isotonic}} - \tau_{\text{isometric}} \dot{=} 0.1 \text{ sec}$$

Figure 3. Ideal Crossover Model

full attention tracking operations the pilot will adjust his gain to offset any variation in controlled element gain in order to maintain a nearly fixed control system bandwidth. Thus the full-attention closed-loop bandwidth ω_c (identified as the crossover of the 0 dB gain line with the K/s amplitude ratio plot) is independent of the controlled element gain. Furthermore, the pilot tends to keep the product of the crossover frequency and the task RMS error, $\omega_c \sigma_e$, constant.

In the crossover model the exponential term with time delay τ approximates all the lag contributions due to pilot and vehicle high frequency dynamic modes. The effective time delay is a function of, among other things, the force/displacement characteristics of the manipulator. As shown in Fig. 3, an isometric (force) stick results in less lag than does an isotonic (free moving) stick. Past experimentation¹³ has identified the difference to be approximately 0.1 sec.

In Fig. 3 if the pilot gain were set at the value represented by K_{p2} with an isometric stick, the bandwidth would be indicated by ω_{c2} and would result in a system stability phase margin, ϕ_{m2} , and gain margin, GM. If this same gain were employed with the isotonic stick, the phase margin would be 0, and a low frequency continuous oscillation (PIO) would result. This oscillation can then be alleviated by pilot gain reduction to the value represented by K_{p1} , thereby accepting a reduced bandwidth. Thus Fig. 3 can be used to demonstrate the common low frequency PIO problem which generally occurs in the vicinity of 0.5 Hz and which is relieved by reducing pilot gain. (In the crossover model an ω_u of 4 rad/sec corresponds to $\tau = \pi/2\omega_u = 0.4$ sec for the total pilot, control system, aircraft, etc., latency).

Limb-Sidestick Neuromuscular Model (and Its Implications). As previously noted, early studies on the neuromuscular system noted the presence of a neuromuscular system or limb-manipulator peak at 14-19 rad/sec well past the usual "crossover region."⁷ The effects of various restraints on the limb/neuromuscular system include closed-loop neuromuscular system model fits to pilot/controlled-element describing function measurements for pressure and free moving manipulators.⁸ An important part of the neuromuscular dynamics in each case is a quadratic mode with damping and natural frequency of

<u>MANIPULATOR</u>	<u>NM/L DYNAMICS</u>
Free Moving	[0.07, 17]
Isometric or Pressure	[0.138, 18.6]

There is also a neuromuscular system mode which is approximated by a first-order lag break at about 10 rad/sec. This mode is also somewhat dependent on the nature of the manipulator restraints.^{13,14}

The reason that the neuromuscular actuation system dynamics differ when the manipulator restraints are changed is physiological -- the neuromuscular

apparatus involved depends on the restraints and limb movements. While greatly oversimplified, the neuromuscular actuation elements of the human may be viewed as a two loop system. The inner loop principally involves Golgi, muscle spindle, and other receptors with short pathways directly to spinal level and back to the musculature. Viewed from the output end this loop is primarily sensitive to forces, and because of the short neural pathways the time lags of information flow are small. The effective bandwidth of this loop can, therefore, be quite high. The second or outer loop includes joint receptors as major feedback elements. Their neural pathways, and associated delays, are longer, leading to a lower outer loop bandwidth. In isometric (force-stick) manipulator conditions, there is little or no joint movement, so the inner loop elements should be dominant. With isometric (free-moving stick) conditions, on the other hand, the joint receptors are major elements. As already indicated in connection with Fig. 3 the net difference, in terms of an effective latency, is approximated at low frequencies by a difference in effective τ of about 0.1 sec.

If we now employ the detailed model of the neuromuscular system (instead of only approximating its phase lag contribution as in Fig. 3) and superimpose it on the controlled element K/s as in Fig. 4, we see an open-loop resonant peak in the 2 to 3 Hz frequency range due to the neuromuscular system. The correspondence of the neuromuscular/limb quadratic mode numerical values and observed roll ratchet frequencies is very unlikely to be a coincidence. So, at observed roll ratchet frequencies the neuromuscular/limb mode clearly should be taken into account. Since their primary effect is a resonant peak from which a "Gain Margin" might be measured,* these properties may be of central importance for high gain pilot situations.

EXPERIMENT GOALS AND SETUP

The experimental goals were to investigate and quantify limb/manipulator dynamics and interactions between the neuromuscular subsystem, force sensing side-stick configuration, high gain command augmentation, and command filtering; and to investigate possible relationships between these interactions and the roll ratchet phenomenon. A longer range goal is to provide and enhance guidelines for manipulator-system design.

The experimental setup is depicted in Fig. 5. A roll tracking task was selected in which the pilot matches the bank angle of his controlled element with that of a "target" having pseudo random rolling motions. The random motions are obtained via a computer generated sum of sine waves. The error

*While the "Gain Margin" shown in Fig. 4 indicates the magnitude difference between the $|Y_p Y_c|_{dB}$ peak and the zero dB line, the phase at or near this frequency may differ appreciably from that required for instability. Thus when the "Gain Margin" shown is zero only one of the two conditions for instability may be satisfied. Consequently this is not necessarily a true gain margin in the conventional sense. It does, however, indicate a resonant tendency contributed by the pilot.

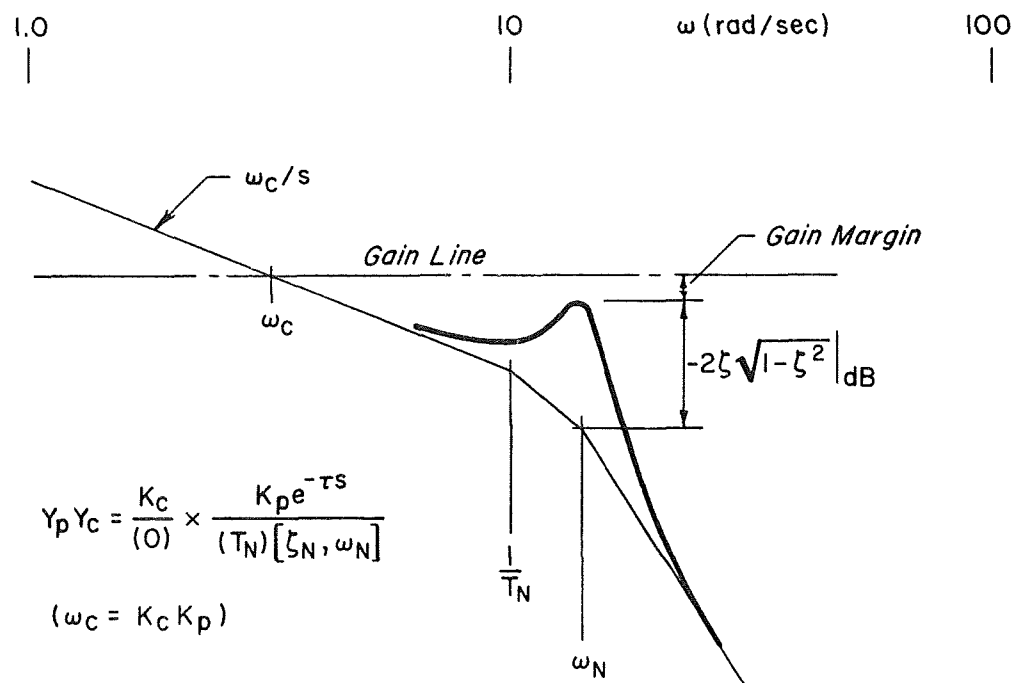


Figure 4. Bode Amplitude Ratio Plot for Neuromuscular System Contribution to Roll Ratchet Potential

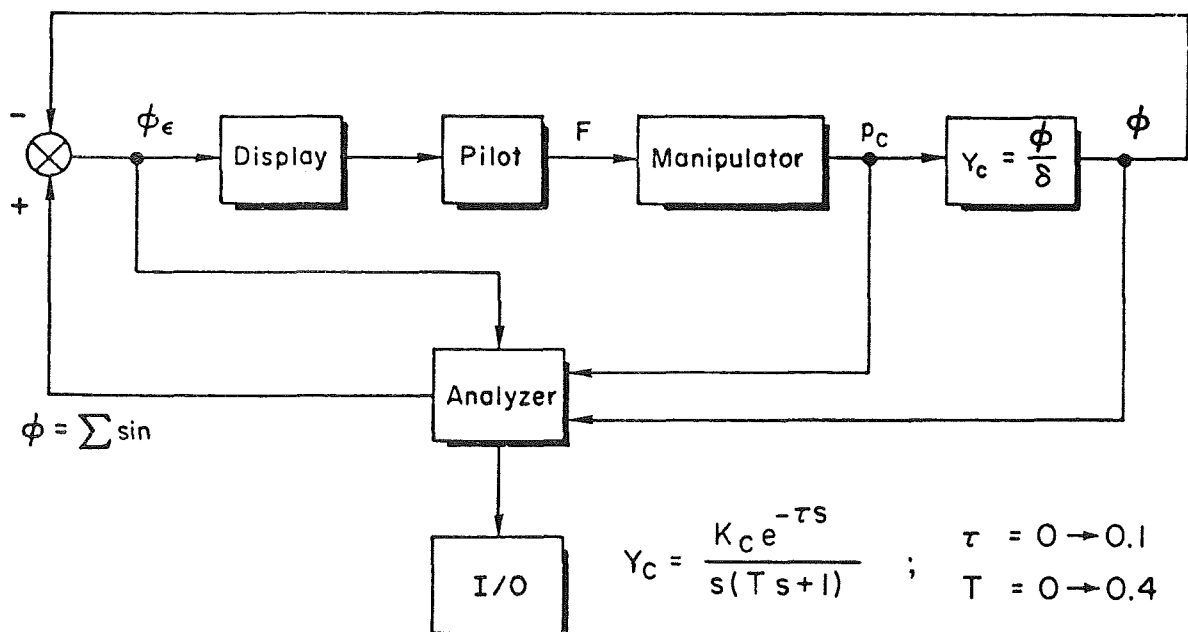


Figure 5. Experimental Setup

is displayed on a CRT and the pilot attempts to null the error by applying force to the manipulator, the output of which becomes the command to the controlled element, Y_C . The form of the controlled element is identified in Fig. 5 along with the range of lag time constants and time delays utilized in the experiment. This controlled element approximates a high gain roll rate command system. The time lag parameter, T , may be considered to be the effective roll subsidence time constant or a flight control system prefilter (between the pilot's stick command and the flight control system), whichever is larger. For very small values of τ the pure time delay may be a realistic approximation to digital flight control system sample and hold dynamics. More generally it is a low frequency approximation for all the high frequency lags in the system which are not covered by the time lag T . Because we are interested primarily in modern flight control systems, the parameter values for T and τ used in the experiment are generally consistent with values that would be present in a system designed to be Level 1 on the basis of flying qualities specifications. Thus, the parameter values used, in the main, should produce excellent effective controlled elements providing the gain is appropriately adjusted.

The manipulator was a McFadden force loader system used in many aircraft research and development simulations. Three stick displacement configurations were employed. One was a fixed (no displacement) stick as in the F-16.¹¹ The second had 0.77 deg/lb (small) stick motion. The third had 1.43 deg/lb (large) stick motion. The latter two matched the displacement/force characteristics employed in an NT-33 flight test.¹² Analog signals from the manipulator force sensor (p_C) and the resulting controlled element roll response ϕ were passed through an A \rightarrow D converter to a digital computer where $Y_p Y_C$ describing functions and various performance measures were computed using STI's Frequency Domain Analysis (FREDA) program. The computations were essentially on-line and printed out at the conclusion of each run. Some 530 data runs were accomplished which provided a tremendous data base from which to determine or identify the various interactions of interest.

No accounts have been found where roll ratchet has been observed or recognized in fixed- or moving-base simulations. It apparently has only occurred in actual flight and then on a more or less random basis. The first objective of this experimental setup therefore was to tune the controlled element, manipulator, and command/force gradients to try to achieve roll ratchet, or at least maximize roll ratchet tendencies, in the fixed-base simulation. A key factor was that describing function measurements must cover the limb neuromuscular peaking frequency region, and forcing functions should be adjusted to emphasize good data in the neuromuscular subsystem region. The experimental runs were accomplished using the summation of sine waves presented in Table 1.

TABLE 1. ROLL TRACKING FORCING FUNCTION

Sine Wave (i)	1	2	3	4	5	6	7	8	9
Frequency (ω_i)	0.467	0.701	1.17	1.87	3.51	7.01	11.2	14.0	18.7
Amplitude (A_i)	15.2	15.2	15.2	7.6	3.04	0.76	0.38	0.228	0.152
Relative Amplitude	1	1	1	0.5	0.2	0.05	0.025	0.015	0.01

$$\phi_I = \sum A_i \cos \omega_i t \quad (\text{deg})$$

EXPERIMENTAL RESULTS

Human Pilot Dynamics

Consistency of Crossover Frequency. It will be recalled that in the ideal crossover model the crossover frequency remains constant even though the controlled element gain may vary. Figure 6 shows results obtained using the fixed side-stick manipulator configuration and a wide range of command/force gradients (controlled element gains). The initial command/force gradients for the F-16¹¹ and the NT-33¹² experimental flight programs are identified for comparison. The controlled element forms range from K/s to $Ke^{-0.07s}/s(0.1s + 1)$. The data for various time delay or time lags are indicated by the symbols. The data points of Fig. 6 indicate two aspects.

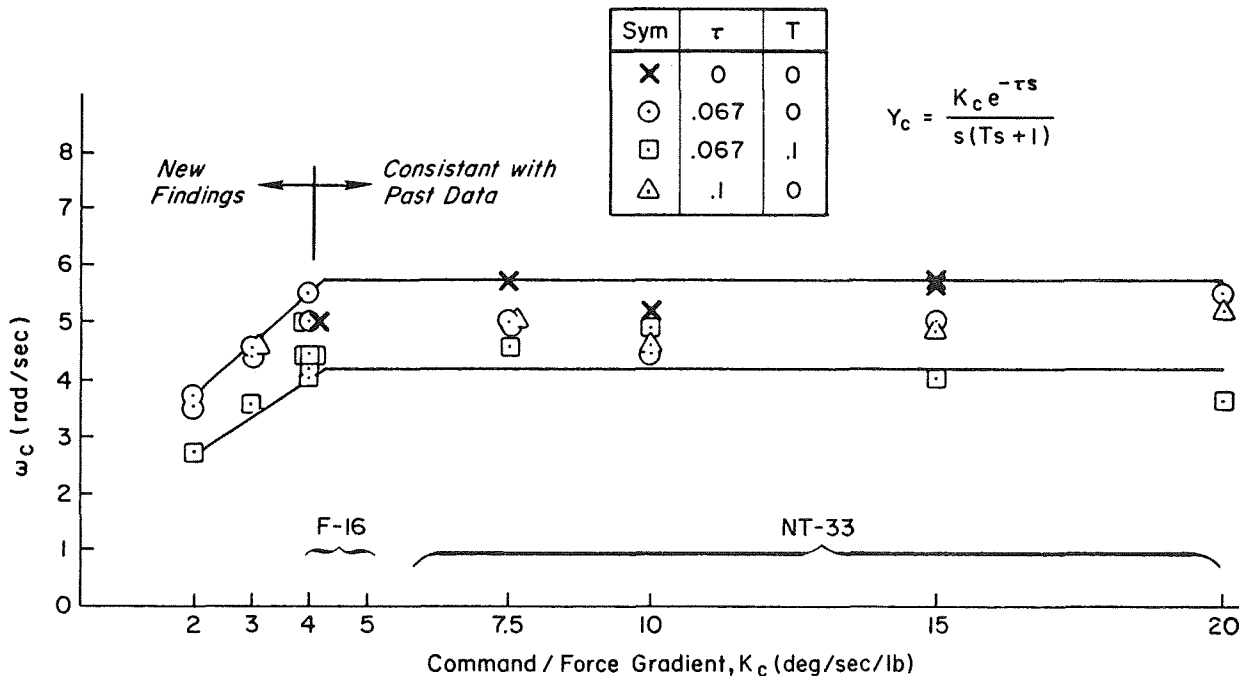


Figure 6. Influence of Command/Force Gradient on Crossover (Fixed Stick)

First they reflect a general decrease in ω_c as controlled element lags increase. Second they show that crossover frequency, as expected, is essentially independent of controlled element gain over a very broad region. But, as the controlled element gain becomes quite low and the manipulator forces required to achieve the desired rolling response become very large, a point is reached where the pilot can no longer accommodate and a rapid drop off in bandwidth results. Interestingly, the F-16 initial command/force gradients lie right at the break in ω_c and therefore represent the lowest values which might be considered acceptable to pilots.

Similar results were obtained with the small and large displacement sidestick configurations except that the crossover frequencies decreased slightly as the displacement was increased.

Neuromuscular System Peaking Tendencies

Turning attention now to the neuromuscular system, Fig. 7 presents the describing function measurements for 3 runs using the fixed force stick and a controlled element having a command/force gradient of 4 deg/sec/lb, no time lag, and a time delay of about 70 ms. The straight line reflects the resulting ω_c/s crossover characteristics. Amplitude departures from this asymptote are the contributions of the pilot's neuromuscular system at high frequency and his trim lag-lead at low frequency. In the region of crossover $Y_p Y_c$ is almost exactly ω_c/s as suggested by the ideal crossover model. The amplitude ratio departures from the asymptote at the highest 3 frequencies shows a peaking in the vicinity of the 14 rad/sec forcing function for 2 of the 3 runs. It also might be noted that there is remarkable consistency in both the amplitude and phase measurements across all frequencies for all 3 runs. In Fig. 7, two of the amplitude data points at 14 rad/sec lie slightly above the 0 dB line. We would therefore expect this to represent a neutral or slightly unstable dynamic mode if the phase angle were near -180 deg at this frequency. This then could be interpreted as affecting roll ratchet.

The two data points at 14 rad/sec are 10 dB above the asymptote and may or may not be exactly the actual neuromuscular system peak, i.e., the peak itself may occur at a slightly higher or lower frequency. The peaking tendency shown in Fig. 7 is representative of a large amount of the data obtained. This frequency is consistent with the roll ratchet frequencies observed in the flight traces.

Influence of Effective Controlled Element Characteristics

The sensitivity of the 14 rad/sec peaking tendency to time delay is shown in Fig. 8. The circles reflect the average values at each frequency and the bars indicate $\pm 1 \sigma$ ranges. The controlled element is $K_c e^{-Ts}/s$. The manipulator is the fixed stick configuration. Results show that a time delay of approximately 0.065 to 0.07 tends to maximize the neuromuscular system peaking. At time delays either below or above these values, the peaking tendency decreases. Of all the controlled elements examined, K_c/s shows the minimum tendency for a peak. Interestingly, the time delay values which maximize the neuromuscular peaking would be considered good from the

ORIGINAL PAGE IS
OF POOR QUALITY

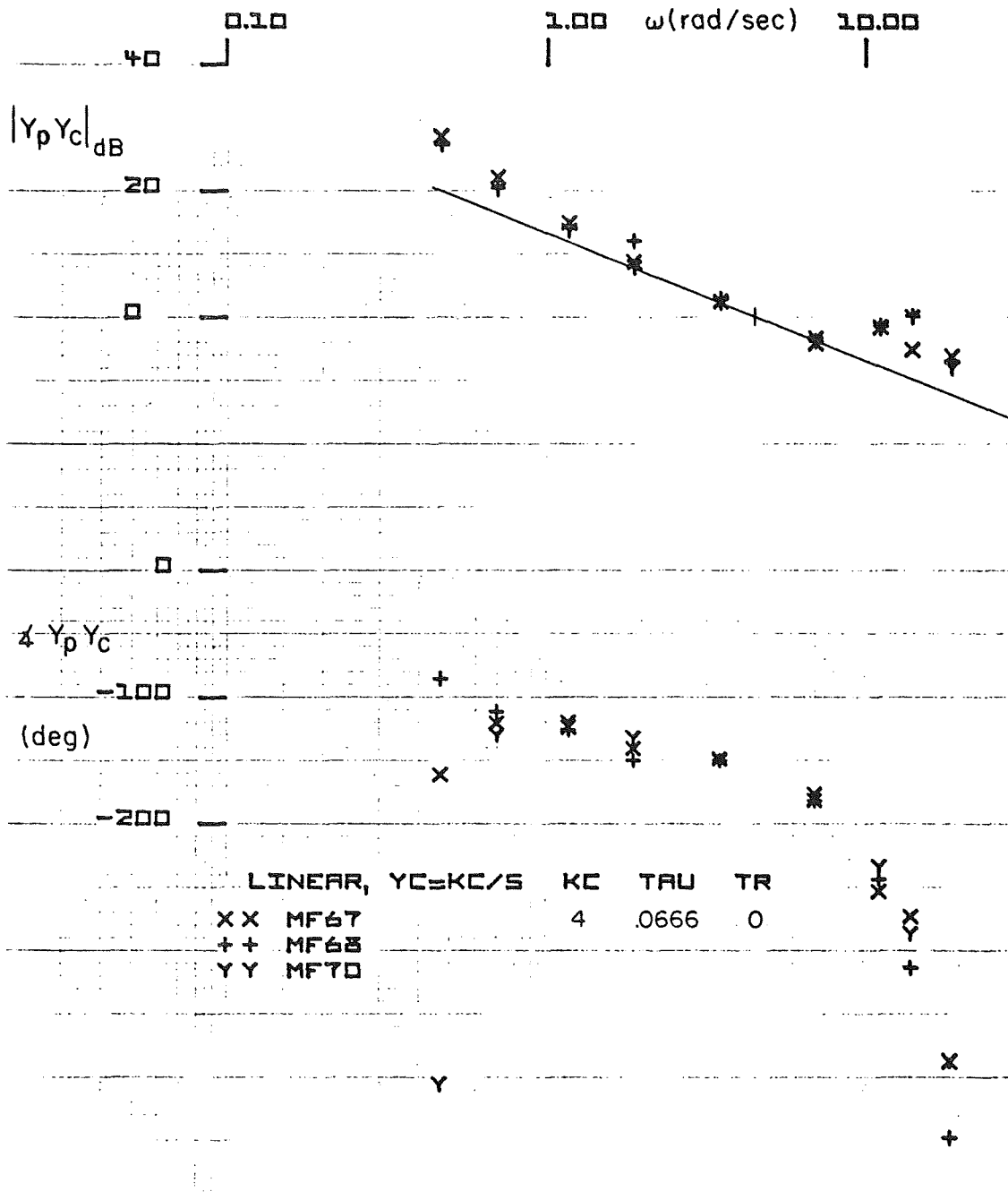


Figure 7. $Y_p Y_c$ Describing Function Amplitude and Phase Plot
for $Y_c = 4/s e^{-0.067s}$

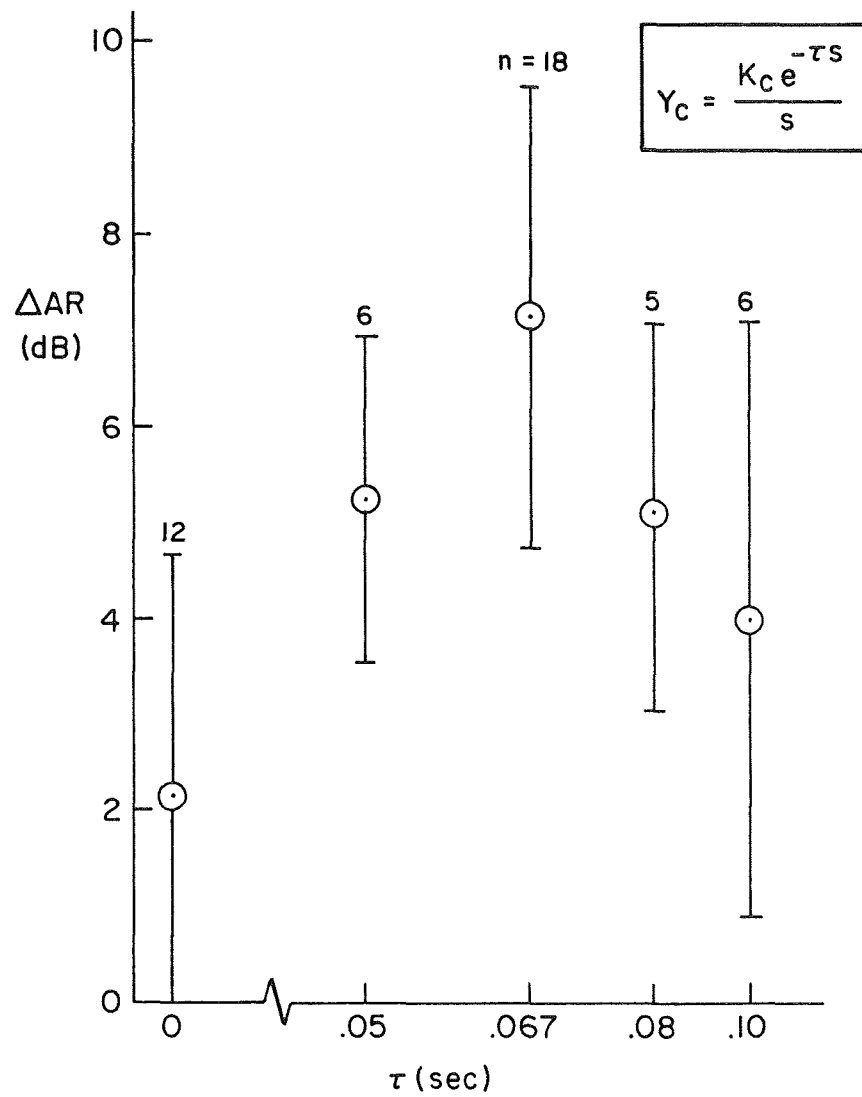


Figure 8. Neuromuscular System Amplitude Ratio Peaking With Controlled Element Time Delay (Fixed Stick)

MIL-8785 flying quality specification standpoint. In essence, these data show that the tendency to peaking can be "tuned" by the adjustment of the controlled element effective lag, with a maximum effect near 0.07 sec.

The neuromuscular system peaking sensitivity to controlled element command/force gradient is shown in Fig. 9. Here the command/force gradient ranges from 3 deg/sec/lb (which is slightly lower than that employed on the F-16) up through 15 deg/sec/lb which was utilized in the NT-33. The data were obtained using the fixed stick and a time delay of 0.067 sec. Data for time lags of 0 and 0.1 have been combined. These data show a slight increase in peaking tendency in the vicinity of 7.5 deg/sec/lb command/force gradient. This is about the same value as the response/force ratio for the Fig. 2 flight traces of ratchet. This may or may not be coincidental. However, it is significant that there is appreciable peaking of the neuromuscular system across the entire gain range investigated in these experiments.

Influence of Stick Characteristics

The influence of stick motion is summarized in Fig. 10. These plots reflect the amplitude ratio peaking at the 3 higher frequencies (11, 14, and 19 rad/sec) for the fixed, the small deflection, and the large deflection stick configurations at 3 different values of the controlled element time delay: 0.0, 0.067, and 0.1 secs. All of these data were taken with the command/force gradient of 10 deg/sec/lb. The results show that there is relatively little difference between the fixed and small deflection force stick. Both show an increase in neuromuscular peaking tendency for the

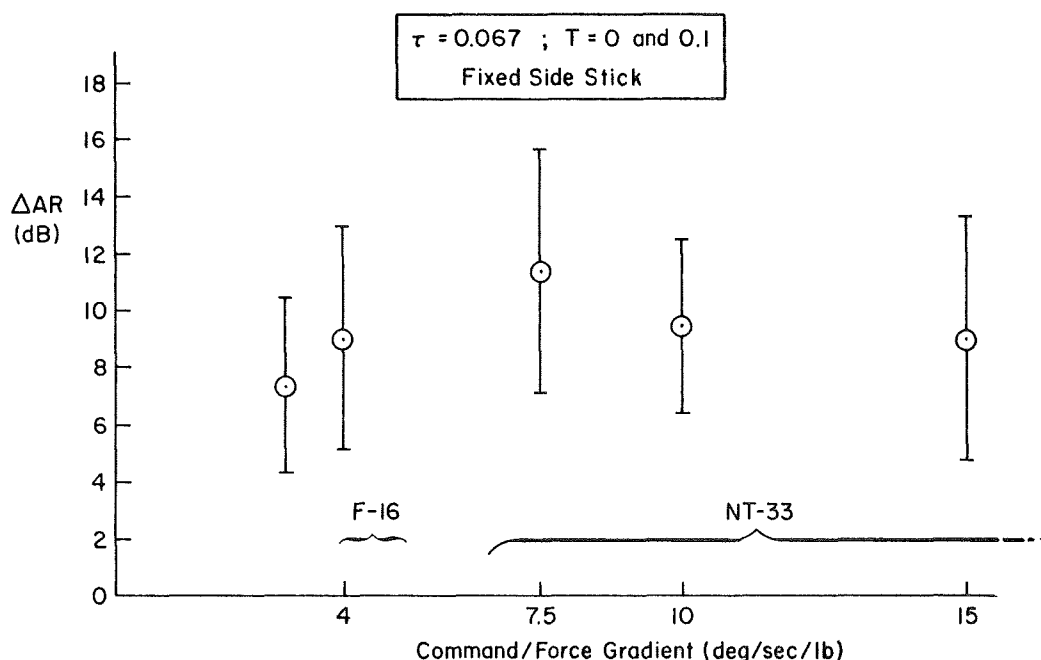


Figure 9. Neuromuscular Peaking Sensitivity to Controlled Element Command/Force Gradient

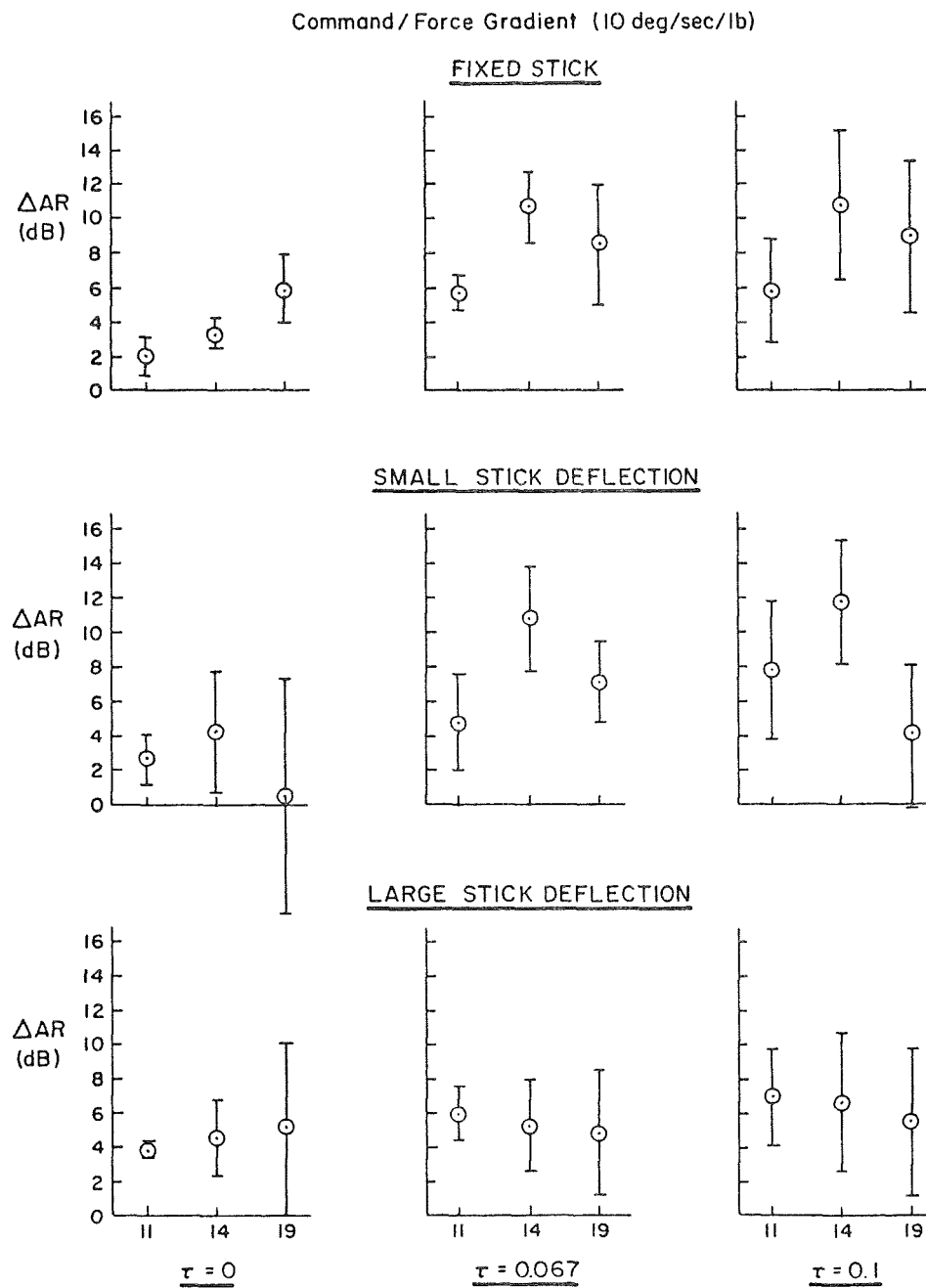


Figure 10. Influence of Stick Displacement on Neuromuscular Peaking Tendency

0.067 and 0.1 sec time delays. They both show a tendency to maximum peaking in the vicinity of 14 rad/sec and in both cases there is considerably less peaking for the zero time delay cases. The large deflection stick, on the other hand, shows a relatively constant amplitude departure from the controlled element asymptote across the 11 to 19 rad/sec frequency band and a lack of sensitivity to the controlled element time delay.

Adjustment of Pilot Lead

The influence of the lag time constant on the neuromuscular system peaking and the possible adoption of lead by the pilot is reflected in Figs. 7 and 11 through 13. Figure 7 shows the neuromuscular peaking obtained with the controlled element command/force gradient of 4 deg/sec/lb, a time delay of 0.067 secs, and no lag. The maximum peaking was noted to be approximately 10 dB and occurred at 14 rad/sec. The addition of a first-order lag time constant of 0.1 sec is shown in Fig. 11. Here the solid line represents the controlled element (Y_c) Bode asymptote adjusted to go through ω_c . The crossover occurs in a region that is K/s in appearance, and the amplitude peaking again is approximately 10 dB, and occurs near the 14 rad/sec data point. The peaks are quite close to the 0 dB gain line, which indicates a likely tendency to roll ratchet. Comparison of the phase plots between Figs. 7 and 11 indicate that the pilot is generating little if any lead to offset the time lag. (Detailed analyses¹⁵ indicate that there is a pilot lead near 8 rad/sec for these cases and for $Y_c = K/s$ which tends to compensate for the high frequency lags in general, but cancels none of them.)

In Fig. 12 the time lag has been moved to 0.2 secs. Comparison of the phase angle data points in Figs. 7 and 12, or Figs. 11 and 12, indicates that the pilot has introduced lead in the Fig. 12 case which essentially cancels the time lag at 0.2 secs. The asymptote for the Y_p/Y_c open-loop system is thus represented by the solid line below the time break point and the dashed line above that break point. Again the amplitude ratio is ω_c/s -like in the vicinity of the crossover. However, there is now considerable scatter in the data points in the region of the neuromuscular system peaking dynamics. In only one of the three runs shown in Fig. 12 was there a peaking tendency for the neuromuscular system and this appears to be concentrated in the vicinity of 11 rad/sec rather than the 14 as noted previously. In the other two runs, the amplitude data points lie quite closely to the Y_p/Y_c asymptote.

In Fig. 13 the lag time constant has been moved down to 0.4 sec. Again comparison of the phase plots shows that the pilot has now moved his lead down to precisely cancel the controlled element time lag contribution so that the resulting Y_p/Y_c has the appearance of an ω_c/s throughout the frequency region of interest. The peaking tendency of the neuromuscular system is no longer evident and there should be little chance of roll ratchet. However, the roll control bandwidth has now been reduced to approximately 2.5 rad/sec whereas it was approximately 4.5 rad/sec with the time constant of 0.1 sec. If the pilot were to attempt to achieve a 4.5 rad/sec bandwidth in the presence of the lag characteristics shown in Fig. 13, a PIO would

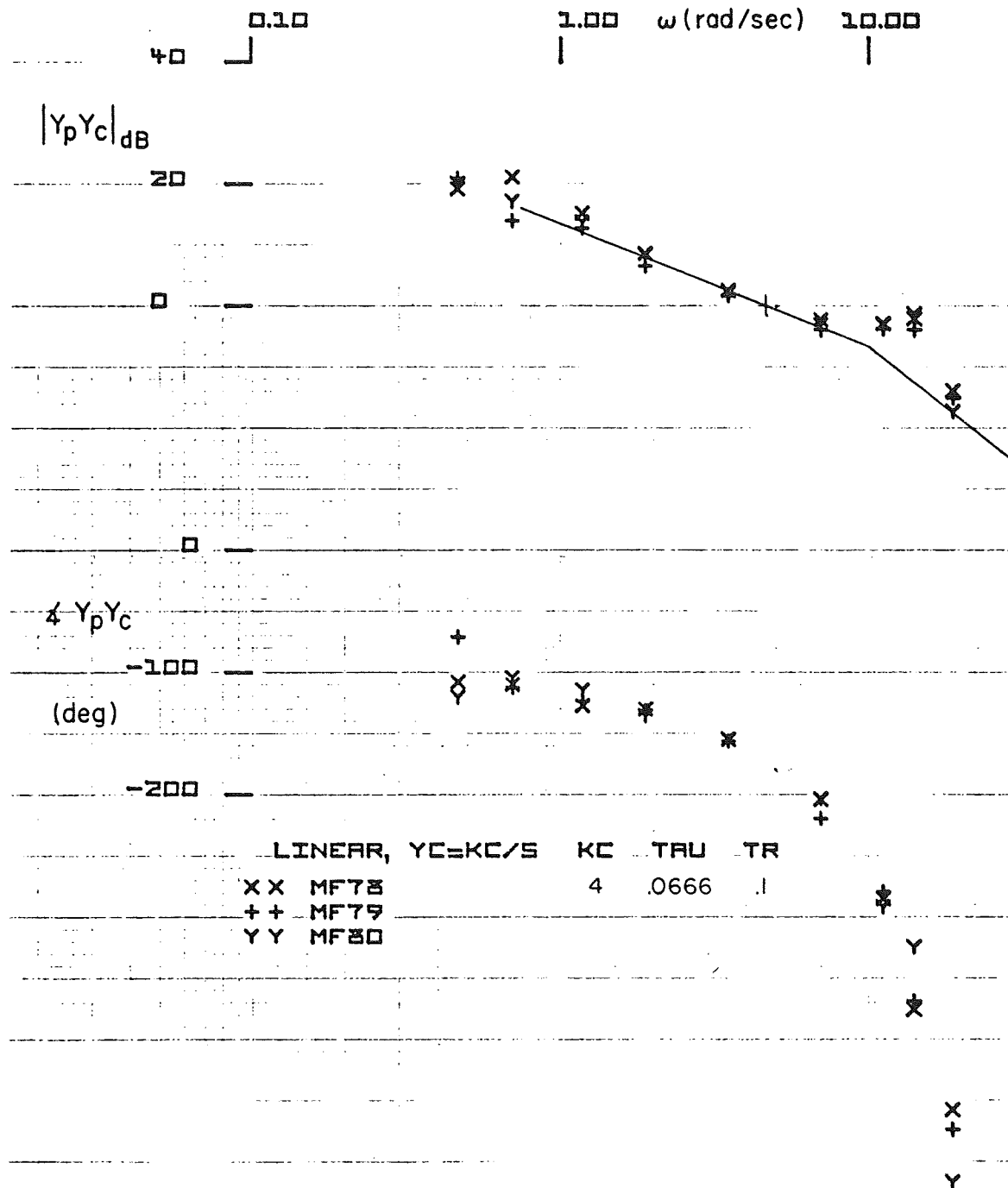


Figure 11. $Y_p Y_c$ Describing Function Amplitude and Phase Plot

$$\text{For } Y_c = \frac{4e^{-0.067s}}{s(0.1s+1)}$$

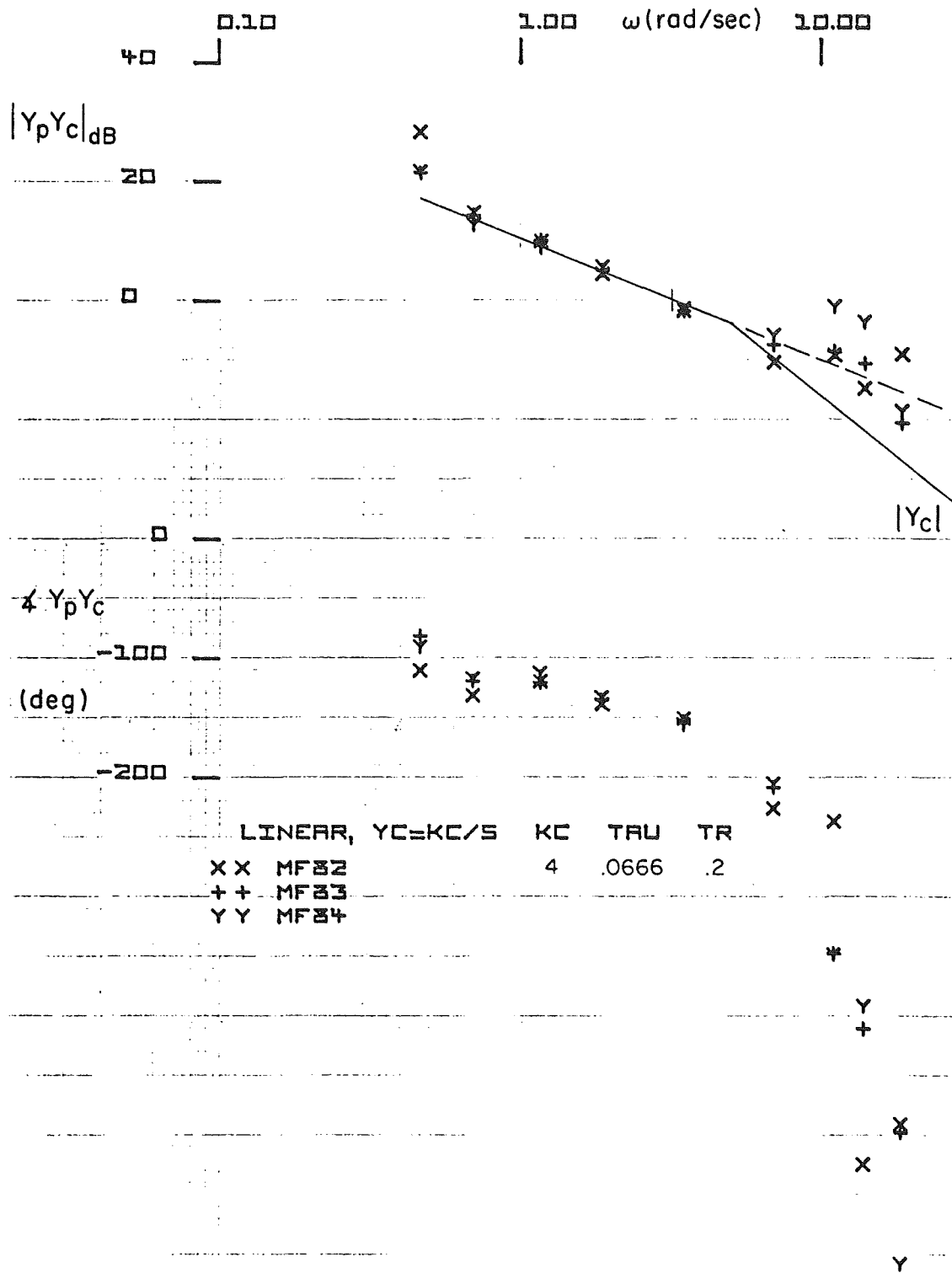


Figure 12. $Y_p Y_c$ Describing Function Amplitude and Phase Plot

$$\text{For } Y_c = \frac{4e^{-0.067s}}{s(0.2s+1)}$$

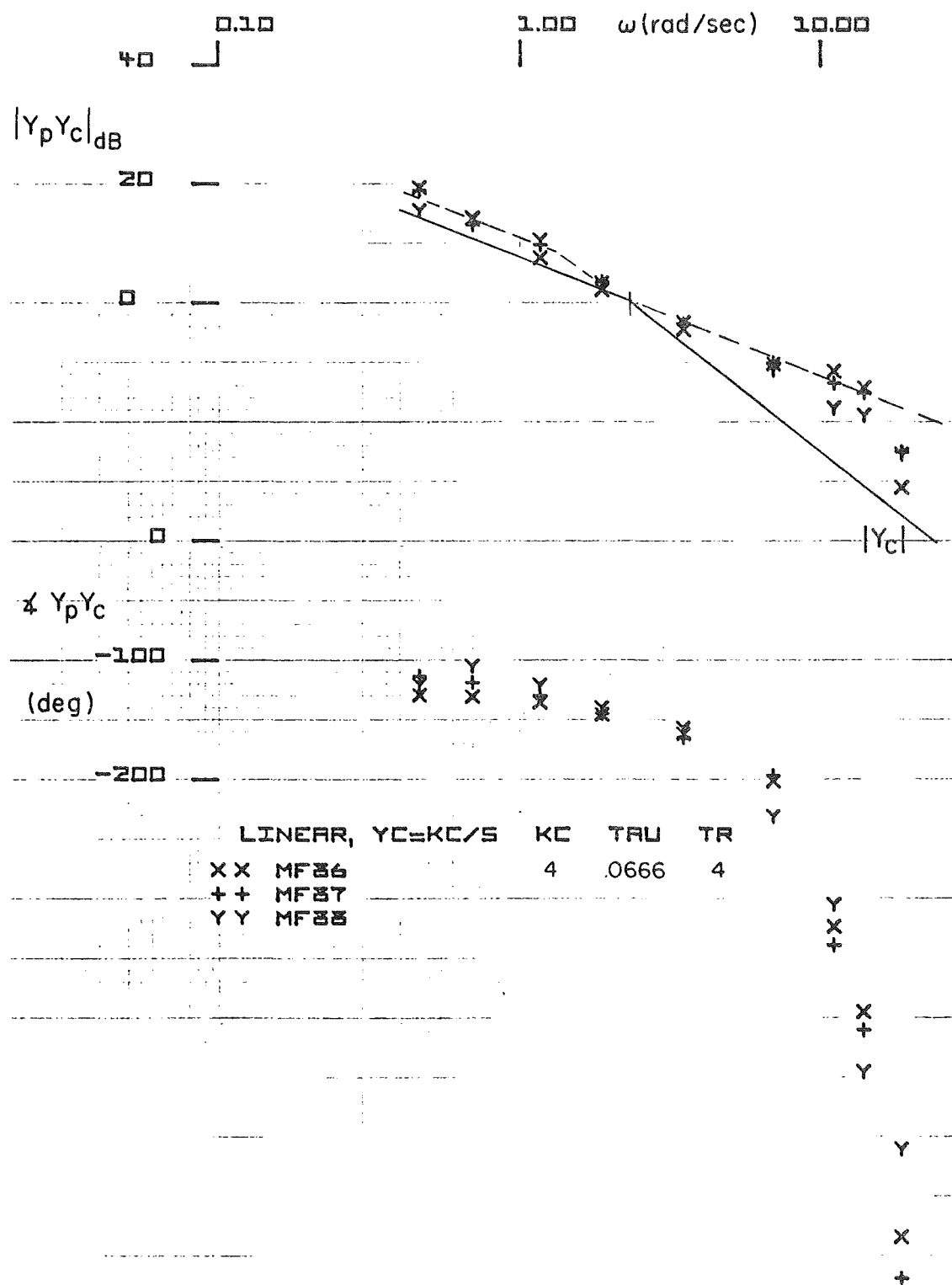


Figure 13. $Y_p Y_c$ Describing Function Amplitude and Phase Plot

$$\text{For } Y_c = \frac{4e^{-0.067s}}{s(0.4s+1)}$$

occur at roughly that frequency (4 rad/sec). Thus in reducing or eliminating the roll ratchet tendency, we may have substituted a tendency for the lower frequency PIO.

Closed-Loop Pilot-Vehicle System Characteristics

Observed Fixed-Base Roll Ratchet. The previous sections have emphasized the neuromuscular peaking tendency as a harbinger of the roll ratchet phenomenon. Yet, in the data presented, the open-loop system phase angle has generally been greater in magnitude than -180 degrees. This means that the gain differences between the peak and the 0 dB line are not necessarily true gain margins. The closed-loop pilot-vehicle systems will, therefore, not necessarily show an oscillation at the neuromuscular peaking frequency although the resonant peak will ordinarily be indicated in the closed-loop system. The pilot remnant, being relatively broadband in character, will therefore act as a driving mechanism to excite the resonant peak.

In some cases the experimental data actually indicated a roll ratchet-like oscillation under conditions similar to those where the phenomenon was found in flight. Most commonly these were stretches in the time histories which involved nearly steady-state rolling velocity commands. An example is given in Fig. 14. Here a short segment of the roll attitude command input is nearly triangular, and the pilot's stick force trace indicates a 2-3 Hz oscillation. Because the forcing function is a random appearing time signal, with only very occasional segments akin to the triangular or steady rolling commands shown, this type of ratchet-like pilot output trace is atypical in the context of a total experimental run. The pilot subjects, in fact, did not report that they had encountered the condition since it was so transitory. Yet it appeared quite commonly once the conditions were favorable -- i.e., neuromuscular peaking tendency present and momentarily steady rolling velocity command. Consequently the fixed base simulation can be said to have successfully demonstrated roll ratchet-like phenomena.

Fixed Force Stick Tracking Task

$$K_c = 3, \tau = 0.067, T = 0.1$$

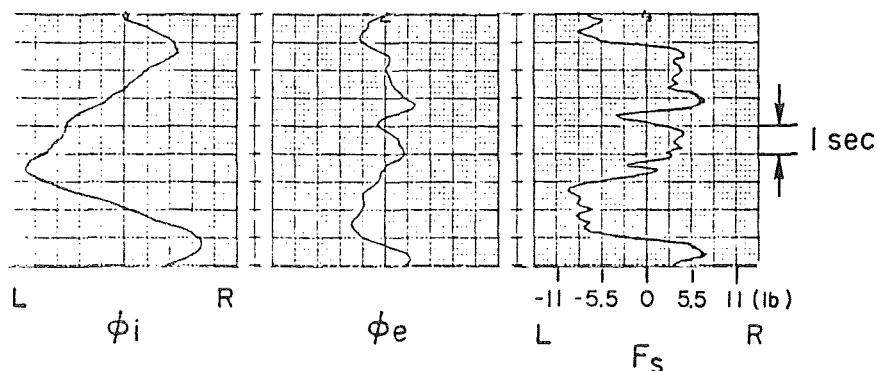


Figure 14. Example of Roll Ratchet-Like Oscillation in Stick Force Trace

It is also useful to re-examine the open-loop describing function data when a first-order correction is made to the data to account for the effect of rapid rolling motion on the pilot during flight. The pilot's angular motion sensing neurological apparatus acts very much like a rate gyro inner loop in the frequency range near and slightly above crossover.¹⁰ This inner loop, present when superthreshold rolling velocities are imposed on the pilot, has the effect of reducing the effective time lags in the pilot's visual-input/manipulator output response. The reduction can be as much as 0.1 second from the fixed-base data. When changes of phase lag of the magnitude 0.1ω are made on typical describing function data showing major neuromuscular peaking, the net phase shift in the frequency region about the peak is very often near -180 degrees. Figure 15 shows a typical example for the fixed force stick configuration with $T = 0$, $\tau = 0.067$, and $K_C = 10$ deg/sec/lb. Therefore one can conclude that the fixed-base neuromuscular peaking examples which show negative gain margins of the amplitude ratio peak relative to 0 dB are quite likely to result in oscillations in the flight situation. The roll ratchet phenomenon in these cases would therefore be high-frequency PIO's which intimately involve the pilot's limb-manipulator neuromuscular system dynamics.

Comparisons with Flight Data

The controlled elements in Figs. 11-15 essentially duplicate the F-16 configurations tested¹¹ and the qualitative results and trends are the same. The compromise selection for the prefilter in the F-16 was a time constant of 0.2 rad/sec which is shown in Fig. 12 to allow a comfortable bandwidth slightly above 3 rad/sec and having 30 to 35 deg of phase margin and a much reduced neuromuscular peaking tendency. Thus there should be minimum tendency for either low or high frequency PIO although the data scatter in the higher frequency range of Fig. 12 show that conditions favorable to roll ratchet could pop up from time to time.

Yet another comparison between simulation results and flight data can be drawn from the investigation of roll ratchet and various prefilter configurations flown in the NT-33.³ In this case one set of effective controlled elements are a close match to this simulation. A major difference, however, was the use of a center-stick in the NT-33. The roll ratchet encountered in this flight test was described as "response which was objectionably abrupt, resulting in a very high frequency, pilot-induced-oscillation (wing rocking) or having 'square corners' or being very 'jerky.'" The frequency was approximately 16 rad/sec.

Figure 16 is a replot of data from Ref. 6 with command/force gradient plotted versus the roll time constant, T_R . The circles identify configurations flown; the open symbols reflect no ratchet obtained, the shaded symbols reflect roll ratchet observed by one or more of the evaluation pilots over the range of time delays investigated. (It should be noted in passing that in almost every case, the ratchet only occurred with non-zero τ as was the case in the lab simulation.) The triangular symbol at $T_R = 0.2$, $K_C = 12.5$ is another NT-33 data point obtained from a flight program in which the roll time constant was selected at 0.2 sec for up-and-away tasks and 0.5 sec for landing tasks.¹² In addition, two 20 rad/sec first-order filters were

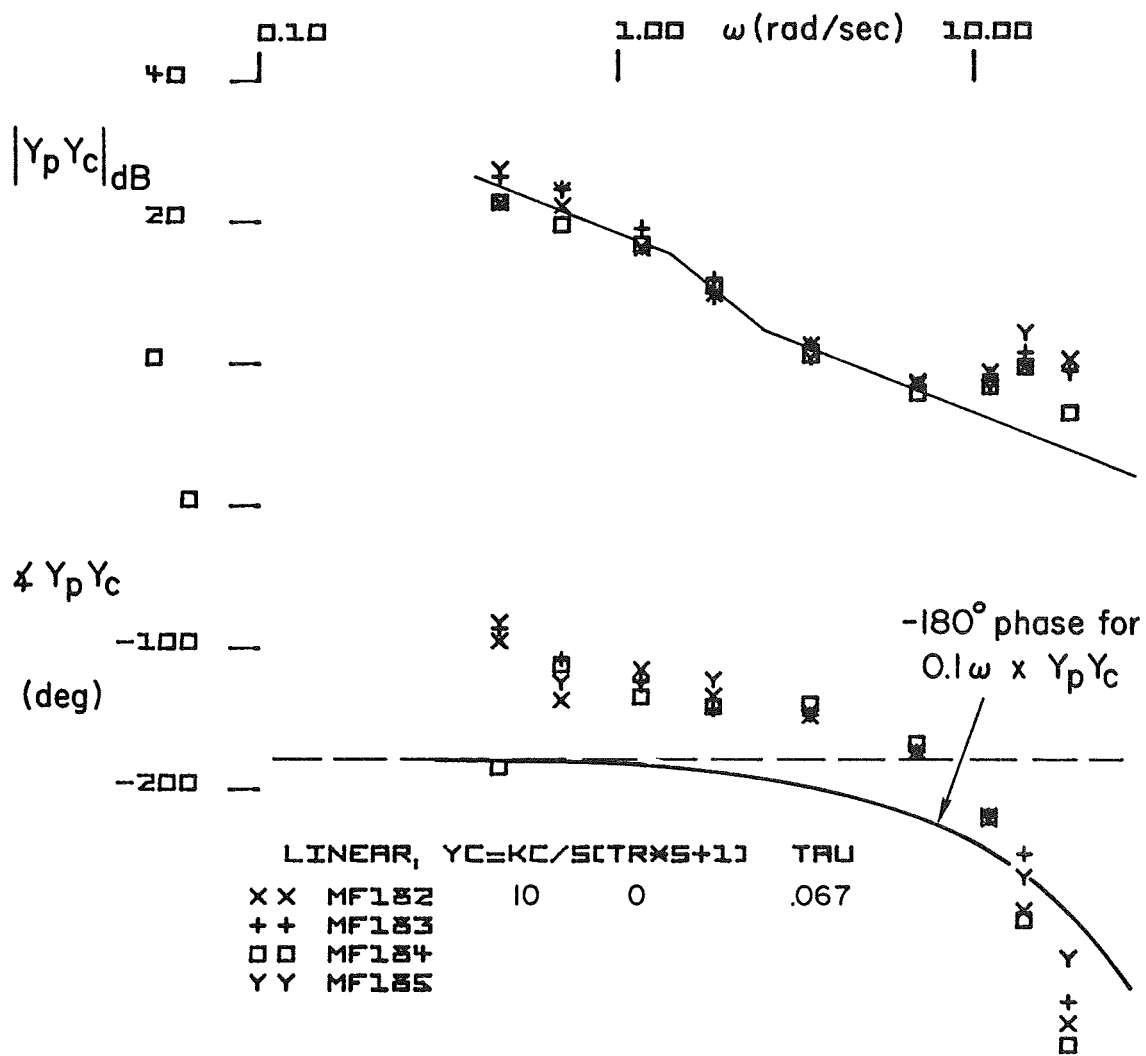


Figure 15. Expected Phase Shift Due to Motion Effects

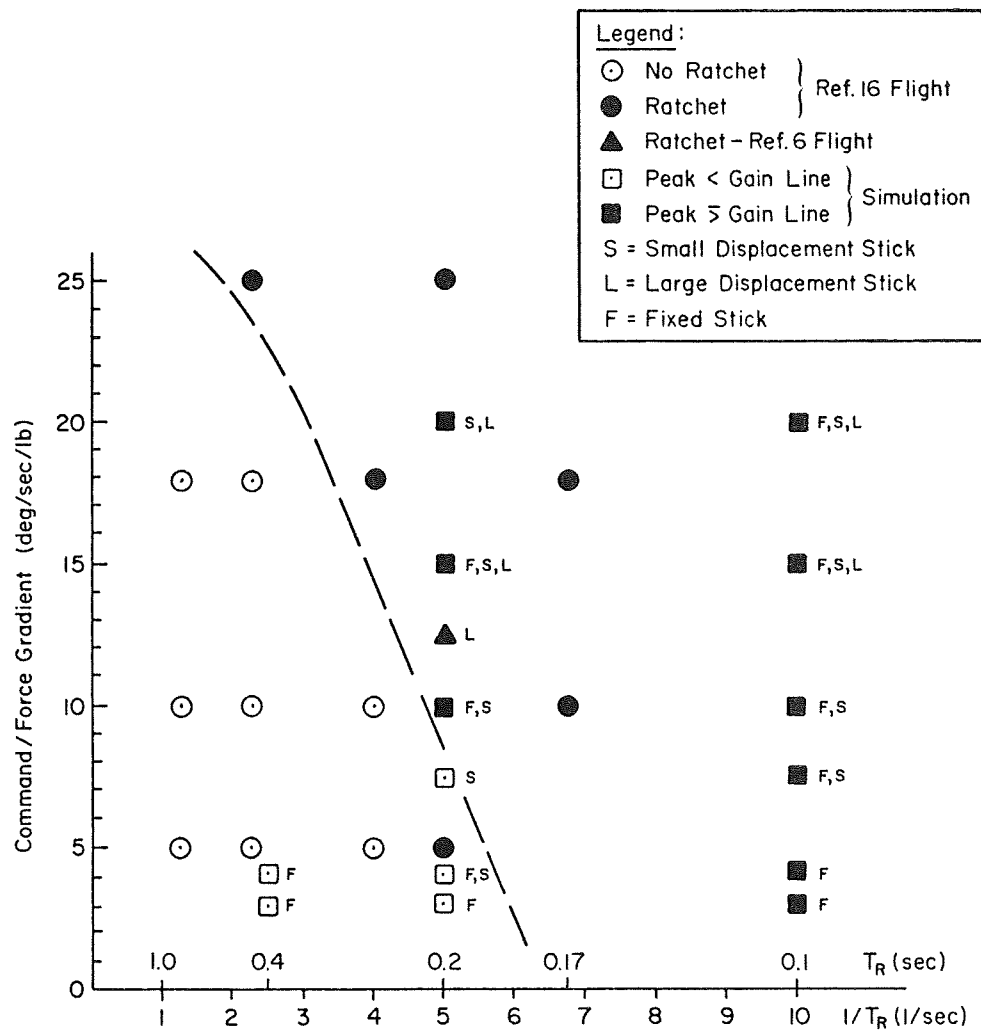


Figure 16. Roll Ratchet Comparison, Flight and Simulator

included in the roll rate command prefilter to "eliminate high frequency noise." Even so, this one case of ratchet tendency was observed.

The square symbols in Fig. 16 are configurations investigated in the fixed-base simulation. The open symbols identify configurations for which the $Y_p Y_c$ zero dB line did not pass through the neuromuscular peak (no ratchet possibility). The shaded squares identify configurations for which the zero dB line passed through the peak (ratchet possibility). The letters F, S, L reflect the displacement of the simulator side-stick. It is likely that the L side-stick most closely matched the NT-33 center-stick characteristics.

There is very good correlation between the flight and lab simulation ratchet tendencies shown in Fig. 16. The dashed line appears to separate the non-ratchet from the ratchet configurations except for the two or three lowest command/force gradient configurations at $T_R = 0.2$ sec. It is possible that this difference may be related to wrist (simulation side-stick) versus arm (flight center-stick) neuromuscular subsystem contributions at the lower command (higher force) configurations. The good agreement between flight and simulator results is interpreted as an encouraging validation of the simulator definition of ratchet potential -- i.e., neuromuscular peaking cut by the $Y_p Y_c$ zero dB line.

Pilot-Manipulator System Asymmetries

It was noted in the discussion of the influence of the command/force gradient on crossover in Fig. 6, that the control bandwidth ω_c decreased markedly as the command/force gradient decreased below 4 deg/sec/lb. The reason for this can be observed in the time traces of Fig. 17. The trace on the left is the random rolling motion of the target. The trace in the middle is the roll error between the target and the controlled element, the trace on the right is the stick force input to the controlled element. It will be noted on the force trace that in roll to the right the stick force rarely exceeds 5.5 lbs, but in rolls to the left the force frequently is as high as 8 lbs and shows a maximum peak at 11 lbs. This is consistent with the commentary^{3,11} where the pilots indicate difficulty in generating rolls to the right using the thumb, but have little difficulty in rolls to the left where they can use the entire palm of their hand to generate the force. Thus we see bi-modal control in the traces of Fig. 17 with larger magnitude, shorter duration forces in rolls to the left and lower magnitude, longer duration forces being used in rolls to the right. Notice that the roll error average is approximately zero in the middle trace. Thus the area under the force traces for left vs. right maneuvers must be approximately the same. For right rolls, lower forces are held for longer periods of time. This results in a lower crossover or bandwidth for right rolls as compared to left rolls and hence a lower average bandwidth for the run. This bi-modal control characteristic was most evident for the 3 deg/sec and 4 deg/sec/lb controlled element or command force gradients, but was also evident up as high as the 7.5 deg/sec/lb. Thus the reduced bandwidth shown in the Fig. 6 plots for the low gain systems. For higher command/force gradients, the forces employed in the tracking task were sufficiently low that there was little difference between left and right maneuvers.

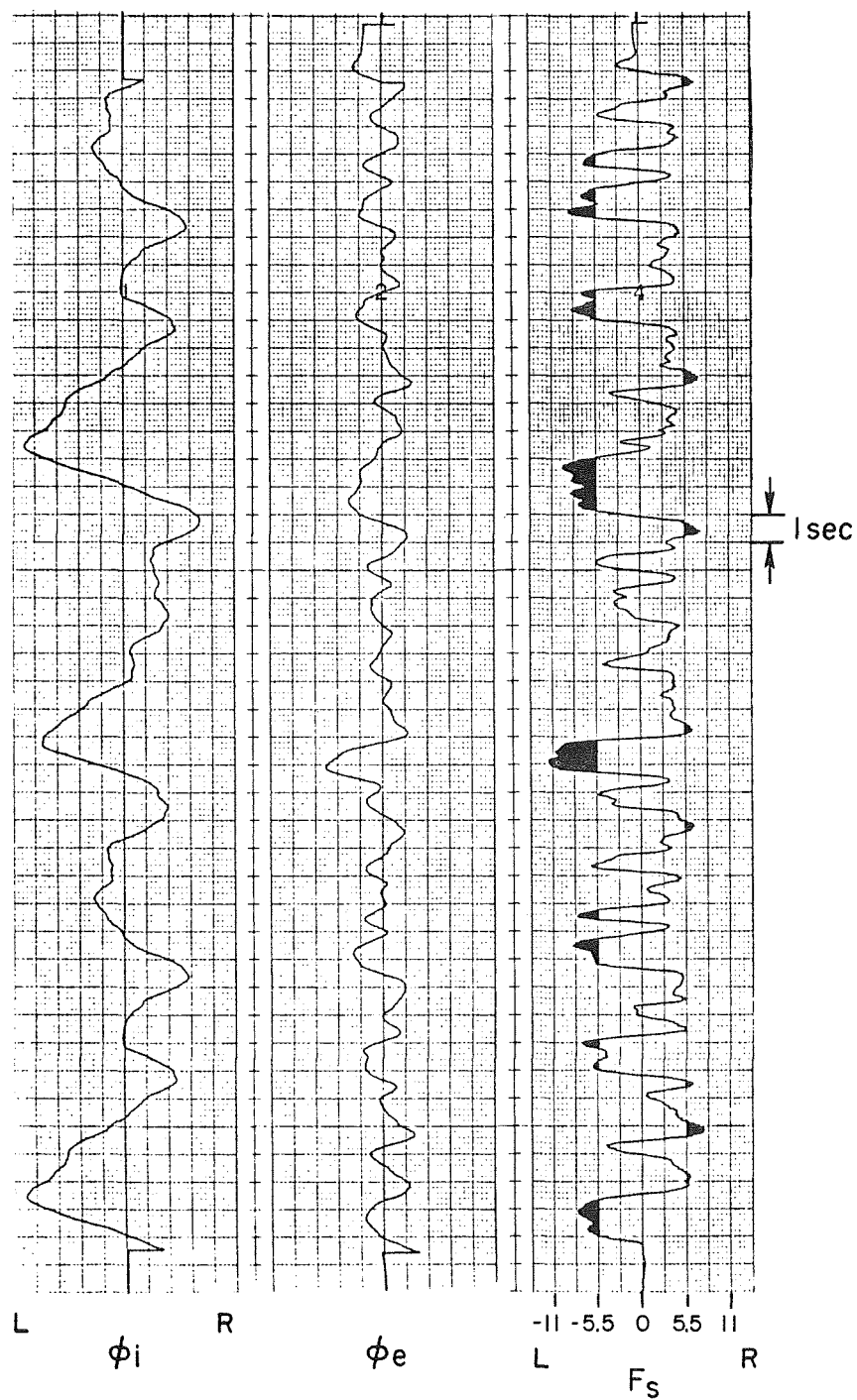


Figure 17. Time Traces of Fixed Force Stick Tracking Task
Run 115, $K_c = 3$, $\tau = 0.067$, $T = 0.1$

CONCLUSIONS

This fixed-base experimental investigation has identified and quantified interactions between the pilot's neuromuscular subsystem and such aspects of typical modern, high response, roll rate command control system mechanizations as:

- side-stick type manipulator force/displacement configuration
- command augmentation forward loop gain
- controlled element effective lag time constant
- flight control system effective time delay

The simulation results provide insight to high frequency roll ratchet oscillations, low frequency PIO, and roll-to-right control and handling problems previously reported in the production F-16, NT-33 side-stick, and NT-33 roll rate command augmentation investigations. The experimental configurations encompass and/or duplicate a number of actual flight situations and have reproduced control problems observed in flight.

Specific conclusions relating to human pilot dynamic characteristics and possible connection to roll ratchet are summarized in the following.

Human Pilot Dynamic Characteristics

1. Crossover Model Refinements

- The property $\omega_c(Y_c) = \text{constant}$ extends over an order of magnitude variation in K_c changes in force gradient. ω_c begins to fall off as very small K_c demand great pilot effort (large K_p) to keep ω_c constant.
- Controller element lags for $Y_c = K_c/(Ts + 1)$ are:
 - almost exactly cancelled by pilot lead when $T > 0.2$ second (lag breakpoint of 5 rad/sec);
 - partly offset by pilot lead of approximately 1/8 second when $T \leq 0.2$ second.

Thus the adjustment rule indicating that pilot lead will offset controlled element lags by nearly exact cancellation now has a lower limit at about 1/8 second.

2. Human Pilot Limb-Manipulator Dynamics

- The classical third-order system approximation for the limb-manipulator portion of the human neuromuscular system is both adequate and an essential minimum form needed to consider pilot-aircraft system dynamic interactions in the frequency range from 8-20+ rad/sec.
- The peaking tendency (damping ratio, ζ_N) of the quadratic component of the third-order approximation is a very strong function of the controlled element dynamics -- in essence this feature can be "tuned" by adjusting controlled element properties.
- For all stick force/displacement characteristics investigated the highest ζ_N (smallest peaking tendency) occurred for $Y_c = K_c/s$ controlled elements.
- Pure time delay induces a greater peaking tendency than an equivalent time lag.
- Distinct peaking tendencies occurred for fixed and small stick deflections for $\tau = 0.07$ and 0.1 second.
- The controlled element form which exhibited the maximum peaking tendency ($\Delta AR = 7$ dB) was $Y_c = K_c e^{-\tau s}/s$, for $\tau = 0.07$ sec. Higher and lower values of τ resulted in less peaking.
- For large stick deflections the peaking tendency is minimized or non-existent.

Roll Ratchet Connections

- The data strongly support the suggestion that the roll ratchet phenomenon is a closed-loop pilot-vehicle system interaction in which the pilot's neuromuscular dynamics play a central role.
- Ratchet tendencies can be detected in fixed-base simulations by careful tailoring of the forcing function and examination of particular stretches of data. Unlike the case in flight, the pilot may not be aware of the occasional ratchet.

- ③ The ratchet potential of a given configuration is associated with the degree of neuromuscular system peaking. This peaking tendency can be "tuned" or "detuned" by controlled adjustments in the effective vehicle dynamics.
- ③ This is readily assessed in a fixed-base simulation by describing function measurements in tracking tasks conducted with an appropriate forcing function. Such procedures are recommended as pre-flight development tests with modern fly-by-wire command augmentation systems.
- ③ Ratchet tendencies are most severe on force sensing sidestick manipulators with small stick deflections.

ACKNOWLEDGEMENTS

This research was conducted under Contract NAS2-11454 to the NASA Ames Research Center, Dryden Flight Research Facility. The contract Technical Monitor was Mr. Donald T. Berry.

REFERENCES

- ¹Mitchell, D. G., and R. H. Hoh, "Flying Qualities Requirements for Roll CAS Systems," AIAA Paper 82-1356, presented at the AIAA 9th Atmospheric Flight Mechanics Conference, San Diego, CA, 9-11 Aug. 1982.
- ²Harper, Robert P., Jr., In-Flight Simulation of the Lateral-Directional Handling Qualities of Entry Vehicles, Calspan Report No. TE-1243-F-2, Feb. 1961.
- ³Monagan, Stephen J., Rogers E. Smith, and Randall E. Bailey, Lateral Flying Qualities of Highly Augmented Fighter Aircraft, AFWAL-TR-81-3171, Mar. 1982.
- ⁴Smith, R. E., Evaluation of F-18A Approach and Landing Flying Qualities Using an In-Flight Simulator, Calspan Report No. 6241-F-1, Feb. 1979.
- ⁵Chalk, C. R., "Excessive Roll Damping Can Cause Roll Ratchet," J. Guidance, Control, and Dynamics, Vol. 6, No. 3, May-June 1983, pp. 218-219.
- ⁶Allen, R. Wade, Henry R. Jex, and Raymond E. Magdaleno, Manual Control Performance and Dynamic Response During Sinusoidal Vibration, AMRL-TR-73-78, Oct. 1973.
- ⁷Magdaleno, Raymond E., Duane T. McRuer, and George P. Moore, Small Perturbation Dynamics of the Neuromuscular System in Tracking Tasks, NASA CR-1212, Dec. 1968.

- ⁸Magdaleno, R. E., and D. T. McRuer, Experimental Validation and Analytical Elaboration for Models of the Pilot's Neuromuscular Subsystem in Tracking Tasks, NASA CR-1757, Apr. 1971.
- ⁹McRuer, D. T., L. G. Hofmann, H. R. Jex, et al., New Approaches to Human-Pilot/Vehicle Dynamic Analysis, AFFDL-TR-67-150, Feb. 1968.
- ¹⁰McRuer, D. T., and E. S. Krendel, Mathematical Models of Human Pilot Behavior, AGARDograph No. 188, Jan. 1974.
- ¹¹Garland, Michael P., Michael K. Nelson, and Richard C. Patterson, F-16 Flying Qualities with External Stores, AFFTC-TR-80-29, Feb. 1981.
- ¹²Hall, G. Warren, and Rogers E. Smith, Flight Investigation of Fighter Side-Stick Force-Deflection Characteristics, AFFDL-TR-75-39, May 1975.
- ¹³Magdaleno, R. E., and D. T. McRuer, Effects of Manipulator Restraints on Human Operator Performance, AFFDL-TR-66-72, Dec. 1966.
- ¹⁴McRuer, D. T., and R. E. Magdaleno, Human Pilot Dynamics with Various Manipulators, AFFDL-TR-66-138, Dec. 1966.
- ¹⁵Johnston, D. E., and D. T. McRuer, Investigation of Interactions Between Limb-Manipulator Dynamics and Effective Vehicle Roll Control Characteristics, Systems Technology, Inc., TR-1212-1, June 1985 (forthcoming NASA CR).